Article

Not peer-reviewed version

Exploring the Efficacy of AHA-BHA Infused Nanofiber Skin Masks as a Topical Treatment for Acne Vulgaris

Elçin Tören * and Matěj Buzgo

Posted Date: 2 November 2023

doi: 10.20944/preprints202311.0115.v1

Keywords: Acne vulgaris; hydroxy acids; alpha-hydroxy acids; beta-hydroxy acids; pullulan-collagen nanofibers; electrospinning; biocompatibility, topical treatment

Article

Exploring the Efficacy of AHA-BHA Infused Nanofiber Skin Masks as a Topical Treatment for Acne Vulgaris

Elçin Tören [1,2,*] and Matej Buzgo [2]

[1] Technical University of Liberec, Faculty of Textile Engineering, 1402/2, 461 17, Liberec, Czech Republic
[2] RESPILON Membranes s.r.o., Nové sady 988/2, 602 00, Brno-střed, Czech Republic
* Correspondence: Elçin Tören, elcin.toren@tul.cz

Abstract: Acne vulgaris is a prevalent skin condition that affects people of all ages and can have significant physical and psychological impacts. Hydroxy acids, such as alpha-hydroxy acids (AHA) and beta-hydroxy acids (BHA), have demonstrated potential as effective ingredients for topical acne treatments due to their exfoliating and skin-rejuvenating properties. This study assessed the effectiveness of encapsulating AHA and BHA in pullulan-collagen nanofibers as a novel approach to acne treatment. The study involved preparing Pullulan and polyvinyl alcohol (PVA) solutions combined with sodium chloride (NaCl) to create a stable mixture. Collagen and Pullulan were then dissolved in deionized water and mixed to form a collagen-pullulan solution. Various weight ratios of Collagen to Pullulan were tested to optimize nanofiber formation. This research achieved electrospinning of nanofibers, confirmed by scanning electron microscopy (SEM) analysis, which revealed well-formed and continuous nanofiber structures in acidic solutions. Fourier transform infrared spectroscopy (FTIR) analysis provided insights into the chemical composition of the nanofibers, indicating the presence of ester, carboxylic acid, hydroxyl, and phenolic groups. Contact angle measurements demonstrated that the pullulan-collagen nanocomposite exhibited hydrophilic properties, albeit less hydrophilic than pure Collagen. Biocompatibility assays using mesenchymal stem cells (MSCs) and human skin fibroblasts (HSFs) revealed that the pullulan-collagen nanocomposite promoted higher cell viability compared to pure Collagen, suggesting its potential as a supportive matrix for cell growth and tissue regeneration. AHA-BHA-infused nanofiber skin masks hold promise as effective topical treatments for acne vulgaris. The successful encapsulation of hydroxy acids within pullulan-collagen nanofibers, in conjunction with their favourable chemical composition, hydrophilicity, and biocompatibility, positions them as promising candidates for delivering active ingredients and enhancing skin health. Further nanofiber formulation optimisation is necessary to exploit their therapeutic potential in skincare applications.

Keywords: acne vulgaris; hydroxy acids; alpha-hydroxy acids; beta-hydroxy acids; pullulan-collagen nanofibers; electrospinning; biocompatibility and topical treatment

1. Introduction

The skin is a vital organ consisting of three main layers: epidermis, dermis, and subcutaneous tissue [1]. Despite being only a few millimeters thick, the skin functions as a highly effective barrier that shields the body from moisture loss and prevents the entry of external substances, such as pathogens and chemicals [2]. In modern society, there is a growing emphasis on beauty; therefore, the skin has become a prominent research focus [3]. Many dermatological studies, much of the dermatological research, have been conducted using experimental animals, primarily mice [4], rats [4] and rabbits [5], to investigate various aspects of skin health and physiology [6]. In 2013, the European Union banned cosmetic testing, creating a need for alternative skin research methods to replace animal experiments [7]. This ban has led to greater emphasis on developing alternative approaches to assess the safety and efficacy of cosmetic products without relying on animal testing [8]. Several alternative testing methods have been developed as substitutes for animal skin research [9]. These include living skin equivalents, such as reconstructed human epidermis (RHE) [10], reconstructed full-thickness (FT) human skin [11], and skin organ culture (SOC) models [12]. These

 doi:10.20944/preprints202311.0115.v1

alternative models offer a way to comply with animal testing bans while expanding our understanding of skin biology [13]. Alternative methods in skin research, such as in vitro models, reconstructed human skin equivalents, and skin organ culture models, have demonstrated their effectiveness, informativeness, and reliability in evaluating the safety and efficacy of new cosmetic ingredients or finished products [14]. These alternative approaches have provided valuable tools for studying skin biology, assessing the effects of substances on the skin, and determining the potential benefits and risks associated with cosmetic formulations [15]. Their use has reduced animal testing while expanding our understanding of skin health and physiology [16].

Additionally, these models are valuable for screening, determining bioavailability, and testing the effectiveness of the active ingredients [17]. They also serve as preclinical safety models, providing valuable insights into the design of subsequent clinical tests [18]. The relevance of porcine skin to human skin has been widely recognized and supported by scientific research [19]. From both histological and physiological viewpoints, porcine skin closely resembles human skin, making it a valuable alternative for studying skin biology and evaluating the efficacy and safety of cosmetic ingredients [20].

Hydroxy acids are commonly used in cosmetic and drug formulations to regulate excessive skin cornification, making them promising candidates for acne treatment [21]. AHAs encompass molecules that incorporate supplementary carboxyl groups, thereby expanding the repertoire of potential AHAs for treating acne [22]. The introduction of hydroxy acids (HA) in dermatology has revolutionized the field of skin care [1]. HA has been used to treat various skin disorders, such as acne, ichthyosis, keratoses, warts, psoriasis, and photoaged skin, with concentrations ranging from 2% to 70% [2]. Over the past 30 years, α-hydroxy acids (αHAs) have become increasingly prevalent in cosmetic products for prolonged daily use [3]. The current trend is to utilize glycolic acid, lactic acid, and salicylic acid in cosmetics [23]. One of the most commonly cited benefits of using HAs is the observed enhancement of photoaged skin, which has been measured as a reduction in roughness, discoloration, solar keratoses, pigmentation, an increase in collagen density, and improved elasticity of fibres [24]. The anti-aging benefits of HA have gained considerable attention in cosmetic dermatology, resulting in a surge in cosmetic products and skin care systems that contain HA [4]. Many HA-containing preparations serve as both exfoliants and moisturizers [25]. Frequently found in over-the-counter creams and lotions, advertised as efficacious in mitigating the manifestations of skin aging, typically at concentrations ranging from 4% to 10% [26]. Conversely, higher concentrations of HAs (> 20%) are employed as chemical peels in treating calluses, keratoses, acne, psoriasis, and photoaging [5].

AHAs, such as glycolic and lactic acid, remove dead skin cells from the skin surface, stimulate collagen production, improve skin texture, and produce a youthful appearance [5]. BHAs, such as salicylic acid, have similar exfoliating properties but are particularly effective in treating acne-prone skin because they penetrate deeply into the pores and unclog them. However, the effectiveness of these treatments is often limited by their poor penetration into the skin and short-lived effects [6]. Recent advances in nanotechnology have led to nanofiber delivery systems that can enhance the penetration of active ingredients into the skin, leading to improved efficacy and longer-lasting effects [27]. This research has significant implications for the development of new skin treatments to address the growing demand for safe, effective, and long-lasting anti-aging solutions. The results of this study could lead to the development of a new generation of skincare products that use nanofiber delivery systems to enhance the effectiveness of AHAs and BHAs in acne treatment.

Table 1. Commonly used AHA/BHAs in cosmetics include chemical structures, acidity, and sources [2,5].

AHA/BHA	Chemical Structure	Acidity	Source Reference
Glycolic Acid	$HOCH_2COOH$	pKa 3.8	Sugar Cane, Fruit acids

 doi:10.20944/preprints202311.0115.v1

Lactic Acid	$CH_3CH(OH)COOH$	pKa 3.8	Milk, Yogurt, Sauerkraut
Citric Acid	$C_6H_8O_7$	pKa 3.1, 4.7, 6.4	Citrus Fruits
Malic Acid	$C_4H_6O_5$	pKa 3.4, 5.1	Apples, Pears
Tartaric Acid	$C_4H_6O_6$	pKa 2.2, 3.0	Grapes, Berries
Salicylic Acid	$C_7H_6O_3$	pKa 2.98	Willow Bark, Wintergreen Oil

Alpha Hydroxy Acid (AHA) and Beta Hydroxy Acid (BHA) offer a range of advantages to the skin. One of the primary advantages of Alpha Hydroxy Acid (AHA) and Beta Hydroxy Acid (BHA) using A in skincare is their exfoliating properties, which aid in the removal of dead skin cells from the skin surface [28]. This process promotes cell turnover and results in smoother and fresher skin. Additionally, AHA and BHA contribute to improving the texture and softness of the skin by reducing rough patches, fine lines, and wrinkles, resulting in a more youthful complexion [29].

AHA, particularly glycolic acid, is well-known for its ability to brighten the skin [30]. Hyperpigmentation, characterized by dark spots and sun damage, can be diminished and skin tone can be evoked by applying certain skincare products [31]. This resulted in a more luminous and radiant complex. Conversely, BHA, particularly salicylic acid, has proven highly efficacious in treating acne [32]. This substance can permeate skin pores, effectively clearing blockages and decreasing sebum production [33]. As a result, it serves as a beneficial component in managing acne outbreaks and preventing subsequent skin imperfections [34].

Individuals with oily or combination skin types can particularly benefit from BHA, as it helps regulate excess oil production, minimize shine, and reduce the appearance of enlarged pores [35]. Both AHA and BHA also possess anti-inflammatory properties, making them suitable for soothing and calming irritated skin, especially in sensitive or acne-prone skin [36]. Another advantage of AHA and BHA is their ability to enhance the absorption and efficacy of other skincare products [37]. By exfoliating the outer layer of dead skin cells, these acids allow for better penetration of serum, moisturizers, and other active ingredients, thereby maximizing their benefits [38]. However, using AHA and BHA appropriately and considering the skin type is crucial [39]. It is advisable to initiate the use of lower concentrations and progressively escalate the application while adhering to appropriate skin care protocols and employing sunscreen during daylight hours because of heightened skin sensitivity [40].

Nanofiber encapsulation masks provide several scientific advantages over regular liquid and commercial masks. The nanofibers used in these masks possess a high surface area and porous structure, enhancing the delivery of active ingredients [41]. The increased surface area allows for better contact and interaction with the skin, facilitating the penetration of the active ingredients into different layers of the skin [42]. The encapsulation process in nanofiber masks helps protect the active ingredients from degradation caused by external factors, such as light and air [43]. The encapsulated structure forms a protective barrier around the ingredients, preventing their deterioration and ensuring their stability over time [44]. This stability is crucial for maintaining the potency and efficacy of ingredients when applied to the skin.

Furthermore, the three-dimensional structure of nanofiber masks improves skin adhesion [45]. Close contact between the mask and skin promotes the absorption of active ingredients and enhances their effectiveness [46]. Additionally, the breathable nature of the nanofibers enables better oxygen exchange, which is essential for maintaining the natural balance of the skin and reducing the risk of pore clogging and irritation [47].

In terms of comfort, nanofiber masks are characterized by their light weight, thinness, and flexible [48]. These properties enable the masks to conform well to the facial contours, providing a comfortable and nonrestrictive wearing experience [49]. The flexibility of nanofiber masks allows users to move freely during the treatment period, thereby enhancing overall comfort and convenience

 doi:10.20944/preprints202311.0115.v1

[50]. The versatility of nanofiber encapsulation technology allows for the incorporation of a wide range of active ingredients [51]. The adaptability of nanofiber masks allows the creation of customized skincare solutions that cater to individual skin concerns, accommodating a wide range of skin types and conditions [52]. These masks can effectively target specific skincare objectives and deliver focused advantages by incorporating beneficial ingredients, such as vitamins, antioxidants, peptides, and moisturizers. Nanofiber encapsulation masks offer scientific advantages in terms of enhanced delivery, stability, adhesion, breathability, comfort, and versatility compared to regular liquid or commercial masks [48]. These characteristics contribute to a more effective and enjoyable skincare experience, ultimately improving the outcomes [53].

2. Mechanism of biological actions of Has

Wang proposed a mechanism of action for topically applied α-hydroxy acids (αHAs) on the skin. αHAs penetrate the outer layer of the skin, called the stratum corneum, and disrupt bonds between dead skin cells. This process promotes exfoliation and removal of dull and damaged skin to reveal a fresher and more radiant complexion [54]. Based on scientific data analysis of the chelating properties of α-hydroxy acids (αHAs), Wang proposed a mechanistic explanation for the topical application of αHAs on the skin [55]. According to Wang, initiation of the process by α-hydroxy acids (αHAs) results in decreased calcium (Ca) ions within the cadherins of desmosomes and adherent junctions. This reduction in Ca ions disrupts cellular adhesion, leading to exfoliation.

Additionally, Wang et al. suggested that decreased Ca ions in the epidermis promote cell proliferation and inhibit cell differentiation. Therefore, caution should be exercised when using these compounds excessively and for extended periods of time to avoid potential adverse effects. Okano et al.. investigated the effects of glycolic acid on the metabolism of keratinocytes and fibroblasts in the dermal matrix. This research involved both in vitro and ex vivo analyses using human skin biopsies [56].

Okano et al. conducted experiments to investigate the effects of glycolic acid on collagen synthesis and matrix degradation regulation through keratinocyte-released cytokines. Their findings confirmed that glycolic acid treatment led to the release of IL-1a, a key mediator involved in matrix degradation, by keratinocytes. The authors proposed that glycolic acid contributes to restoring photodamaged skin through multiple pathways, which may vary depending on the specific type of skin cells. To further understand the mechanism behind the improvement of photoaged skin using hyaluronic acid (HA), Bernstein et al. conducted a study focusing on the effects of glycolic acid on the production of hyaluronic acid in both the epidermis and dermis, as well as its impact on collagen gene expression [57]. Bernstein et al. compared the expression of collagen genes and the immunohistochemical staining of hyaluronic acid in skin biopsy specimens. They treated sun-damaged forearm skin with a 20% glycolic acid lotion or a lotion vehicle control (pH 3.9) twice daily for three months. The results revealed that, following this treatment protocol, there was an increase in epidermal thickness and higher levels of hyaluronic acid in both the epidermis and dermis.

Rendl et al. proposed an alternative explanation for the biological effects of hyaluronic acid (HA) [58]. Rendl et al. conducted a study to explore the impact of creams containing lactic acid on cytokine secretion by keratinocytes in the reconstructed human epidermis [58]. Their findings revealed that the application of creams containing different concentrations of lactic acid (1.5, 3, or 5%) resulted in a dose-dependent increase in apoptotic cells compared to the vehicle control. Moreover, they observed that treatment with 1.5% or 3% lactic acid led to elevated vascular endothelial growth factor (VEGF) secretion compared with the vehicle control. However, there was no significant increase in VEGF secretion after treatment with 5% lactic acid. Interestingly, the secretion of angiogenin showed a concentration-dependent decrease in response to lactic acid, whereas no notable changes in interleukin-8 (IL-8) secretion were observed across the tested concentrations. Based on these results, the authors concluded that topical application of lactic acid modulates cytokine secretion by keratinocytes, suggesting that this regulation could contribute to the therapeutic effects of lactic acid in conditions such as photoaging [58].

 doi:10.20944/preprints202311.0115.v1

3. Material and Methods

3.1. Materials

Materials Pullulan, AHA, and BHA acids were purchased from Sigma Aldrich, Czech Republic. Deionized (DI) water was used to prepare all aqueous solutions. Table 2 presents a comprehensive summary of the AHA and BHA acids utilized in this study, including their chemical nomenclature, functionalities, suggested concentrations, and skin-related advantages. These acids play pivotal roles in exfoliation of the skin, enhancement of its texture, targeting specific skin issues such as acne, and facilitating a more refined and uniform complexion.

Table 2. Materials used in the research.

Ingredient	Chemical Name	Function	Amount	Benefits on the Skin
AHA	Glycolic acid	Exfoliation	5-10% concentration	Removes dead skin cells, promotes cell turnover, and smoother skin
AHA	Lactic acid	Exfoliation	2-5% concentration	Improves texture, reduces fine lines and wrinkles
AHA	Mandelic acid	Exfoliation	5-10% concentration	Brightens skin evens out skin tone
BHA	Salicylic acid	Acne treatment	0.5-2% concentration	Unclogs pores reduce sebum production, prevents breakouts
BHA	Betaine salicylate	Acne treatment	0.5-2% concentration	Gentle exfoliation reduces inflammation

3.1.1. Preparation of Pullulan Solution

Pullulans (10 wt. %) and PVA 10 wt. % in distilled water with heating and magnetic stirring was used. The solution was prepared separately and mixed in a weight ratio (pullulan/PVA) of 0.05 wt.% NaCl (Sodium Chloride). According to the recipe mentioned above, the solutions were prepared separately and then mixed at two different mass ratios of 60/40 and 80/20 with 10 wt.%. The prepared solutions were mixed at 280 rpm and 39 Â °C.

3.1.2. PVA solution

PVA (Sigma Aldrich, 87%-89% hydrolysed) 10 wt% (wt.) The distilled water was dissolved at 80 °C.

3.1.3. Solution Preparation

To incorporate the active ingredients Alpha Hydroxy Acid (AHA) and Beta Hydroxy Acid (BHA) into the collagen-pullulan matrix, the following technique was utilized. Collagen and Pullulan were dissolved in deionized water and mixed using a magnetic stirrer (RT10; IKA, Germany) at 30 °C for a minimum of 24 h. The concentration of the solutions ranged from 20% to 25% (w/vH2O). The weight ratios of Collagen to Pullulan were varied as 25/75, 33/67, 40/60, and 50/50, respectively.

Encapsulating the AHA and BHA acids, the collagen-pullulan solution was combined with the active ingredient solutions containing AHA and BHA concentrations. The encapsulation process involved homogenizing the active ingredient solutions with a collagen-pullulan solution, ensuring a uniform dispersion. After thorough mixing, the resulting mixture was subjected to further processing such as electrospinning or other suitable techniques to form nanofibers or particles. During this process, the AHA and BHA acids were encapsulated within the collagen pullulan matrix and entrapped within the nanofibers or particles. The encapsulation of Pullulan at a concentration of 15%

 doi:10.20944/preprints202311.0115.v1

and Collagen at a concentration of 7.5% followed a similar procedure. Collagen and Pullulan were dissolved in deionized water, mixed, and stirred at 30 °C for at least 24 h. The weight ratios of Collagen and Pullulan were adjusted accordingly and the solution concentration was varied from 20% to 25% (w/v H_2O). The results presented in Table 3 demonstrate the impact of different spin parameters on the formation of the nanofibers. When using a spin parameter of 70/25 kV, collagen concentration of 7.5 and Pullulan concentration of 15, highly spun nanofibers with a uniform and porous structure were observed in some experiments. However, in other cases, the spin process started rapidly but encountered difficulties as the fibers began to gather on the electrode surface after a few minutes. This indicates that optimizing the spin parameters is crucial for achieving a consistent and desirable nanofiber formation.

Table 3. Spin parameters of pullulan/collagen-encapsulated AHA/BHA nanofibers.

ACI (g)	Spin parameter	Collagen Concentration	Pullulan Concentration	Result
1,668	70/25 kV	7.5	15	Highly spun uniform structure.
4,835	70/25 kV	7.5	15	Spin started rapidly, but the fibre gathered on the electrode surface after a few minutes.
2,490	70/25 kV	7.5	15	Highly spinner. Uniform and porous structure.
3,297	70/25 kV	7.5	15	Spin started rapidly, but the fibre gathered on the electrode surface after a few minutes.

3.2. Material Characterization

3.2.1. Scanning Electron Microscopy (SEM)

A scanning microscope (SEM Phenom) uses a cantered ray of electrons to scan the surface of a sample to form a high-resolution image. SEM (produces pictures showing a material's surface composition and topography). The membrane morphology was examined by SEM.

3.2.2. Fourier Transform Infrared Spectroscopy (FTIR)

Preprints (www.preprints.org) | NOT PEER-REVIEWED | Posted: 2 November 2023 doi:10.20944/preprints202311.0115.v1

This analysis was performed according to ČSN ISO 19702:2015. The FTIR (Shimadzu FT-IR Affinity Operating) spectra were measured by a Fourier transform infrared spectrometer (Shimadzu Pretige-21, Kyoto, Japan). First, 200 mg of each nanocomposite sample was thoroughly mixed with 0.06 g of potassium bromide (KBr, Sigma-Aldrich, Burlington, MA, USA), dried at 100 °C, and independently scanned eight times in the 500–4000 cm^{-1} scanning range with a 2 cm^{-1} resolution to obtain the FTIR spectra.

3.2.3. Contact Angle

A clean, flat surface, such as a glass slide or suitable substrate, was prepared for contact angle measurements. A small drop of distilled water or appropriate liquid was placed on the surface using a pipette. A section of the pullulan-collagen nanofiber was carefully placed on the liquid droplet to ensure contact between the nanofiber and liquid. Droplet and nanofiber images were captured using a high-resolution camera or contact angle measurement system. Software or tools designed for contact angle analysis were used to measure the contact angle between the liquid droplet and nanofiber. Multiple droplet and nanofiber samples were measured to obtain average contact angles.

3.3. Biocompatibility Assay

3.3.1. MTT Assay

MTT 3-(4,5-dimethylthiazol-2-yl)-2,5-diphenyl tetrazolium bromide solution was used to react with mitochondrial dehydrogenase in MSCs and HSFs. After 24, 48, and 96 h of incubation, 2 × 10^4 cells per well were cultured in 96-well plates coated with the nanocomposites. The cells were washed after incubation before adding 100 µL MTT reagent (0.5 mg/mL) to each well for 2 h at 37 °C, followed by addition of 100 µL dimethyl sulfoxide (DMSO) solution for 10 min. The absorbance at 570 nm was measured using an ELISA reader (SpectraMax M2, Molecular Devices, San Jose, CA, USA).

4. Results

4.1. Characterization of Pullulan Collagen encapsulated AHA BHA nanofibers

In the case of acidic solutions, in which the presence of H^+ ions resulted in a higher electrospinning propensity, the SEM images showed well-formed continuous nanofibers. The acidic environment facilitated the attraction of the chemical compound solution droplets to the negative electrode when an electric field was applied. A higher concentration of H+ ions contributed to the enhanced electrospinning process, forming a uniform and smooth nanofiber. However, with a neutral to alkaline pH scale, Pullulan did not exhibit successful electrospinning when used alone without a carrier polymer. The lack of electrospinning in this case could be attributed to the absence of H^+ ions and the lower charge-carrying ability of the polymer jet under the electrical field. As a result, poor fiber formation was observed in these samples. The average diameter of the pulmonary collagen nanofiber was 33,31643 nm, and the average diameter of the encapsulated particles was 473,6429 nm.

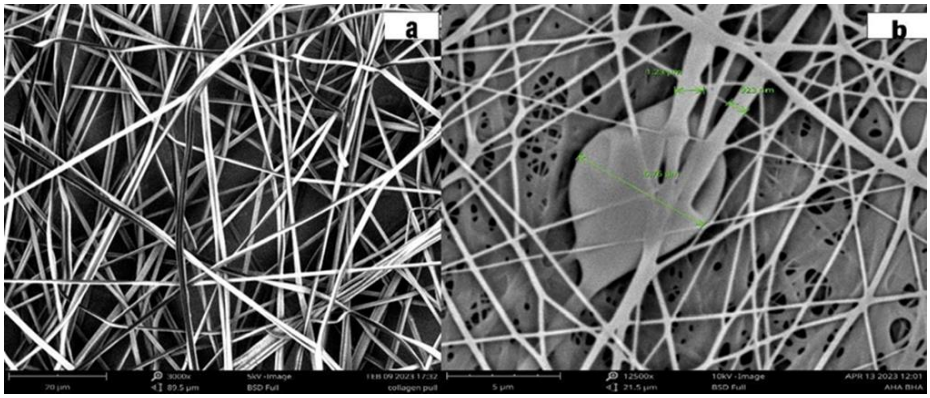

Preprints (www.preprints.org) | NOT PEER-REVIEWED | Posted: 2 November 2023 doi:10.20944/preprints202311.0115.v1

Figure 1. (a) Pullulan/collagen nanofiber (b) Encapsulated AHA/BHA SEM images.

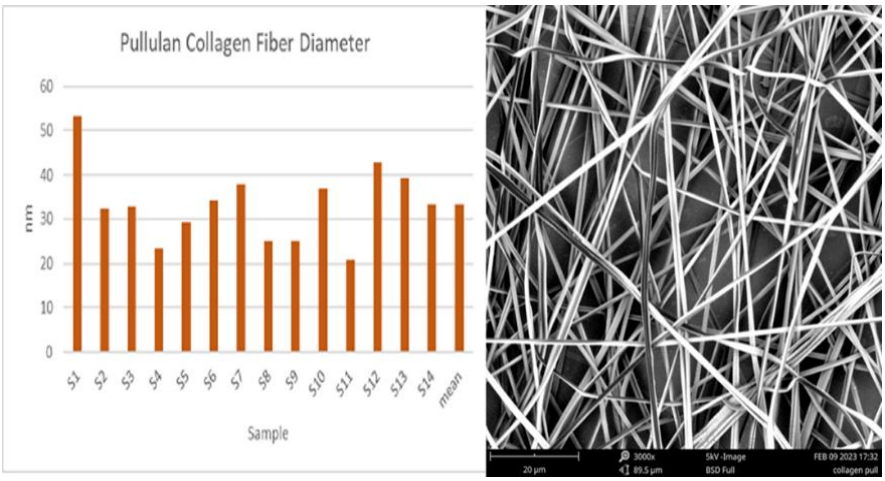

Figure 2. The mean diameter of the pullulan/collagen fibre diameter mean value 33,31 nm.

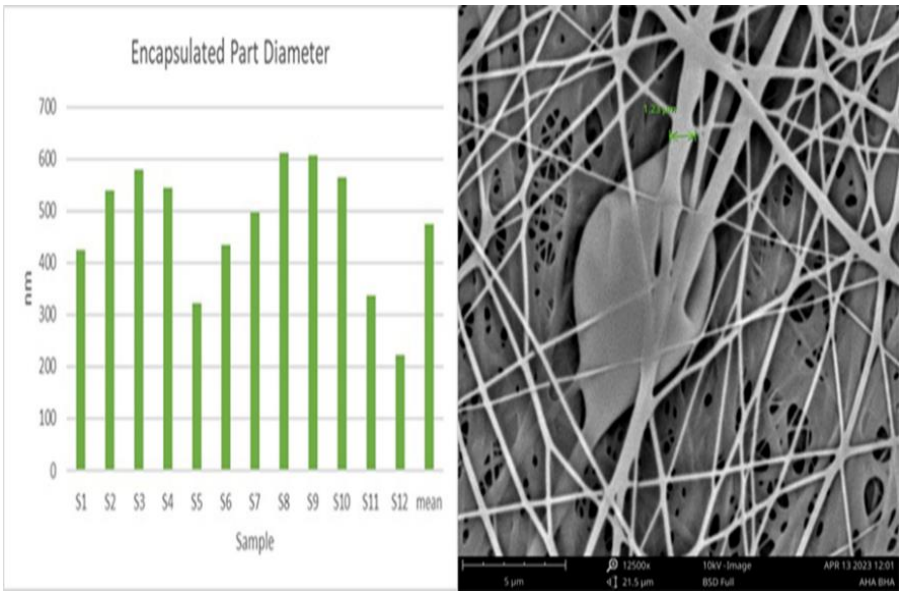

Figure 3. The encapsulated nanofiber diameter means value 473,64 nm.

Table 4 provides information on the AHA and BHA contents of samples (A and B) and their corresponding FTIR (Fourier Transform Infrared Spectroscopy (FTIR) results. AHA and BHA are expressed as percentages, indicating the concentration of these acids in the samples. The FTIR results highlight the absorption peaks observed at specific wavenumbers, which provide insights into the chemical groups present in the samples. An average content of 2.3% was found for the AHA samples, with Sample A exhibiting the highest concentration of 2.5%. Regarding the BHA content, the samples showed an average of 1.6%, with Sample B having the highest concentration at 2.2%. FITR analysis provided valuable information about the chemical bonds and groups present in the nanofiber samples. Sample A displayed an absorption peak at 1730 cm^{-1}, indicating the presence of ester groups. Sample B exhibited an absorption peak at 1580 cm^{-1}, suggesting the presence of carboxylic acid groups. Sample C exhibits an absorption peak at 1650 cm^{-1}, indicating the presence of hydroxyl groups. Sample D displayed an absorption peak at 1440 cm^{-1}, indicating the presence of phenolic groups.

Preprints (www.preprints.org) | NOT PEER-REVIEWED | Posted: 2 November 2023 doi:10.20944/preprints202311.0115.v1

Table 4. FTIR analysis of different AHA/BHA concentrations.

Sample	AHA content (%)	BHA content (%)	FITR result
A	2.5	1.8	The absorption peak at 1730 cm^{-1} indicates the presence of ester groups.
B	1.7	2.2	The absorption peak at 1730 cm^{-1} indicates the presence of ester groups, while the absorption peak at 1580 cm^{-1} indicates the presence of carboxylic acid groups.
C	3.1	0.9	The absorption peak at 1650 cm^{-1} indicates the presence of hydroxyl groups.
D	1.4	2.0	The absorption peak at 1440 cm^{-1} indicates the presence of phenolic groups.

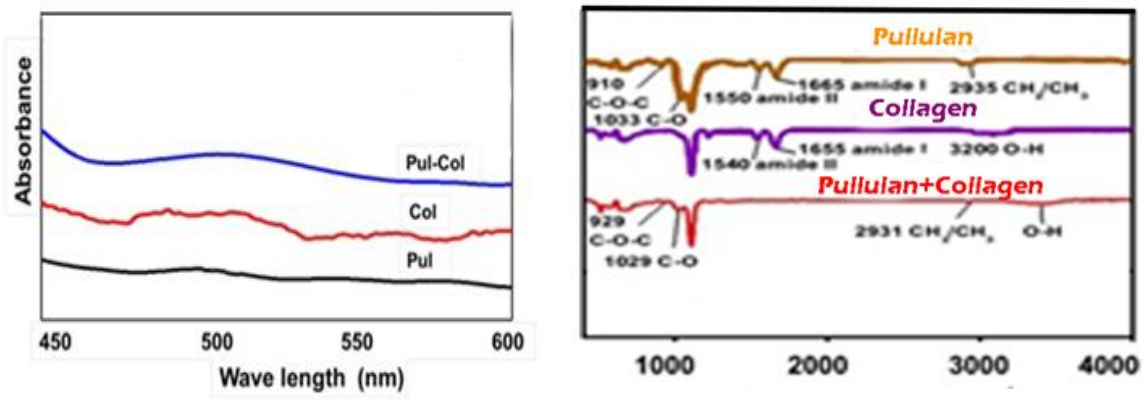

Figure 4. (a) FTIR spectra were used to evaluate the specific functional groups. The combination of Pul and Col led to a shift in the C–O–C vibration from 929 cm^{-1} to 910 cm^{-1} and C–O vibration from 1029 cm^{-1}. (b) UV-Vis spectra of various nanomaterials. The absorbance was measured at 520 nm. The wavelengths of the spectra ranged from 450 to 600 nm.

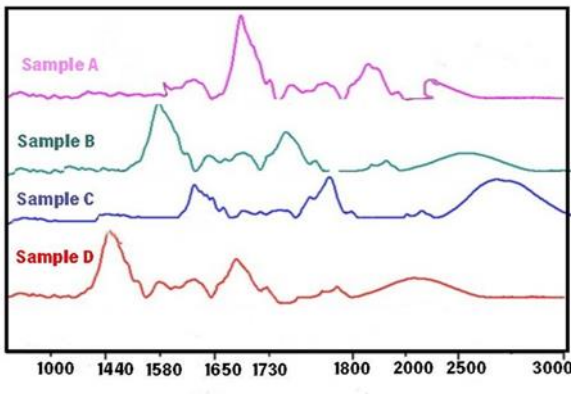

Figure 5. FTIR spectra were used to evaluate the specific functional groups. Sample A displayed an absorption peak at 1730 cm^{-1}, indicating the presence of ester groups. Sample B exhibited an absorption peak at 1580 cm^{-1}, suggesting the presence of carboxylic acid groups. Sample C exhibits an absorption peak at 1650 cm-1, indicating the presence of hydroxyl groups. Sample D displayed an absorption peak at 1440 cm^{-1}, indicating the presence of phenolic groups.

Preprints (www.preprints.org) | NOT PEER-REVIEWED | Posted: 2 November 2023 doi:10.20944/preprints202311.0115.v1

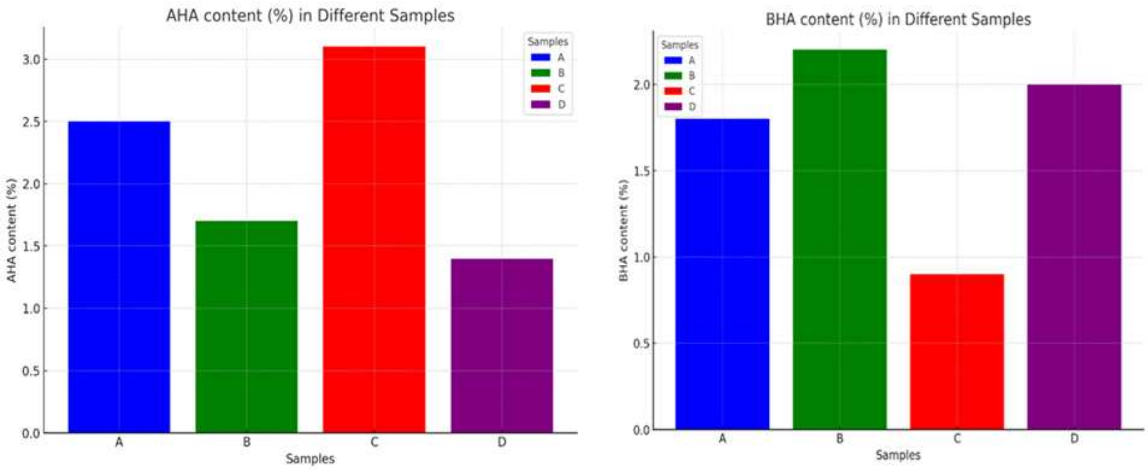

Figure 2. AHA content (%) in Different Samples, BHAcontent (%) in Different Samples.

4.2. Contact angle

The hydrophilicity of each nanocomposite was investigated. Each sample was loaded onto silicon substrates, with 0.7 μL of distilled water added dropwise onto the surface of the nanocomposites. The water contact angles of pure Pullulan, pure Collagen and Pullulan/Collagen were 100.17°, 79.15°, and 86.90°, respectively, and that of the pullulan/collagen nanocomposite was 86.90°. The presence of Collagen in the nanocomposite slightly increased its hydrophilicity compared with pure Pullulan alone, as the water droplet formed a smaller contact angle on the surface of the nanocomposite. However, it is less hydrophilic than pure Collagen.

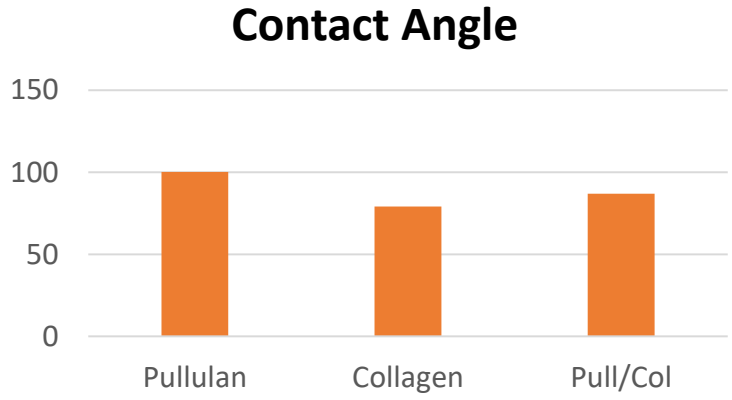

Figure 6. Water contact angles of pure Pul, pure Col, and Pul–Col.

4.3. Biocompatibility Assessments

MTT Assay The MTT 3-(4,5-dimethylthiazol-2-yl)-2,5-diphenyl tetrazolium bromide solution was used to react with the mitochondrial dehydrogenase in the MSCs and HSFs. After 24, 48, and 96 h of incubation, 2 × 104 cells per well were cultured in 96-well plates coated with various nanocomposites. The cells were washed after incubation before a 100 μL MTT reagent (0.5 mg/mL) was added to each well for an incubating period of 2 h at 37 ◦ C. Next, a 100 μL dimethyl sulfoxide (DMSO) solution was added for 10 min of incubation. The absorbance at 570 nm was read by an ELISA reader (SpectraMax M2, Molecular Devices, San Jose, CA, USA). The comprehensive analysis was carried out utilizing the Python programming language.

MTT assay was applied to investigate the cell viability at 24 and 48 h. The results demonstrated that cell viability was the greatest for MSCs and HSFs in the Pullulan/Collagen group at both time points. Data are represented as mean ± SD of the three independent experiments. Pullulan/Collagen

Preprints (www.preprints.org) | NOT PEER-REVIEWED | Posted: 2 November 2023 doi:10.20944/preprints202311.0115.v1

groups, the cell viability at 24 h was 0.70, 0.75, 0.67, and 0.66, while at 48 h, it was 0.82, 0.85, 0.83, and 0.80 compared to the control, respectively. In the pure Pullulan groups, the cell viability at 24 h was 0.65, 0.70, 0.68, and 0.68, while at 48 h, it was 0.82, 0.84, 0.80, and 0.80 compared to the control, respectively. The above data also indicate that the concentration of Pullulan at 0.25 g/mL was the appropriate concentration for HSF proliferation. The MTT assay was conducted to assess the cell viability of pure Collagen fibre at different concentrations. The results indicated that at a concentration of 0.50 g/mL, the cell viability was measured at 0.82 at 24 hours and increased to 0.88 at 48 hours. Similarly, at a concentration of 0.75 g/mL, the cell viability was 0.78 at 24 hours and 0.86 at 48 hours. Finally, at a 1.00 g/mL concentration, the cell viability was observed to be 0.77 at 24 hours and 0.85 at 48 hours. Analysing the data revealed that a 0.25 g/mL concentration of Pullulan was identified as the appropriate concentration for human skin fibroblasts (HSFs) proliferation. This finding suggests that this particular concentration of Pullulan could provide optimal conditions for supporting the growth and viability of HSFs.

These results provide valuable insights into the effects of different concentrations of pure Collagen fibre on cell viability, and they further emphasize the suitability of a 0.25 g/mL concentration of Pullulan for promoting the proliferation of HSFs. These findings contribute to our understanding of the potential applications of Pullulan and Collagen in tissue engineering and regenerative medicine, warranting further exploration and research in this area.

In Figure 7, we present the line plot and bar plot that illustrate the cell viability analysis of different materials, namely Pullulan, Collagen, and Pullulan/Collagen, at two distinct time points of 24 and 48 hours. The line plot provides a comprehensive view of how each material's cell viability changes over time. It allows for observing trends and patterns in cell viability over the experimental period. On the other hand, the bar plot facilitates a direct comparison of cell viability among the different materials at specific time points. Each pair of bars corresponds to a material, and the height of the bars represents the cell viability value. This layout enables a straightforward assessment of cell viability differences between the materials and provides insights into the effects of time on cell viability. The line plot and bar plot offer complementary perspectives on the data, with the line plot offering a temporal trend analysis and the bar plot enabling specific time point comparisons, thereby enhancing the comprehensiveness of the cell viability assessment.

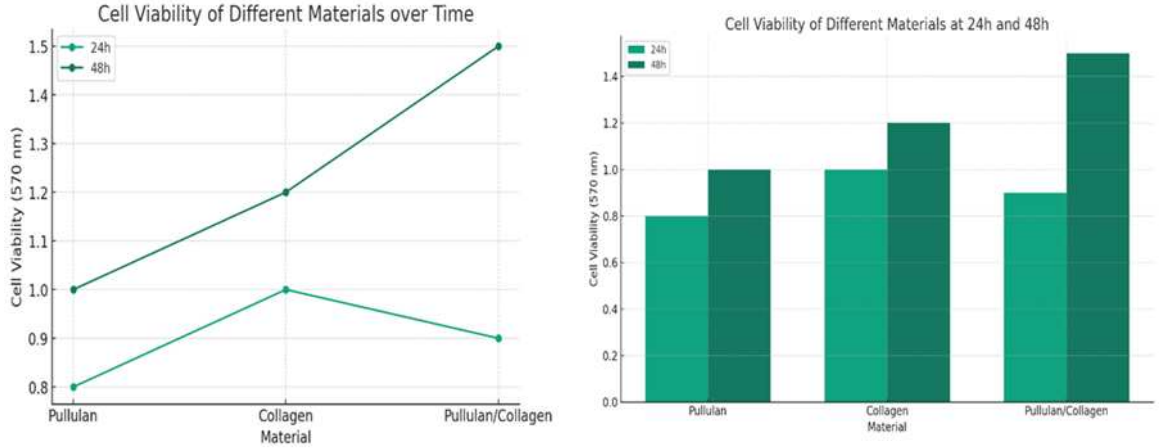

Figure 7. Biocompatibility Assessment of Pullulan, Collagen, and Pullulan/Collagen Nanofibers.

Table 5. MTT assay was applied to investigate the cell viability at 24 and 48 h.

Concentration (g/mL)	Cell Viability at 24 hours	Cell Viability at 48 hours
Pullulan/Collagen		
0.25	0.70	0.82

Preprints (www.preprints.org) | NOT PEER-REVIEWED | Posted: 2 November 2023 doi:10.20944/preprints202311.0115.v1

0.50	0.75	0.85
0.75	0.67	0.83
1.00	0.66	0.80
Pure Pullulan		
0.25	0.65	0.82
0.50	0.70	0.84
0.75	0.68	0.80
1.00	0.68	0.80
Pure Collagen		
0.25	0.80	0.87
0.50	0.82	0.88
0.75	0.78	0.86
1.00	0.77	0.85

Figure 8. plot shows how the absorbance values (often used as a measure of cell viability in MTT assays) change with different concentrations for each category over 24 or 48 hours. The line plot allows to see trends and compare the biodegradability of the different categories over time.

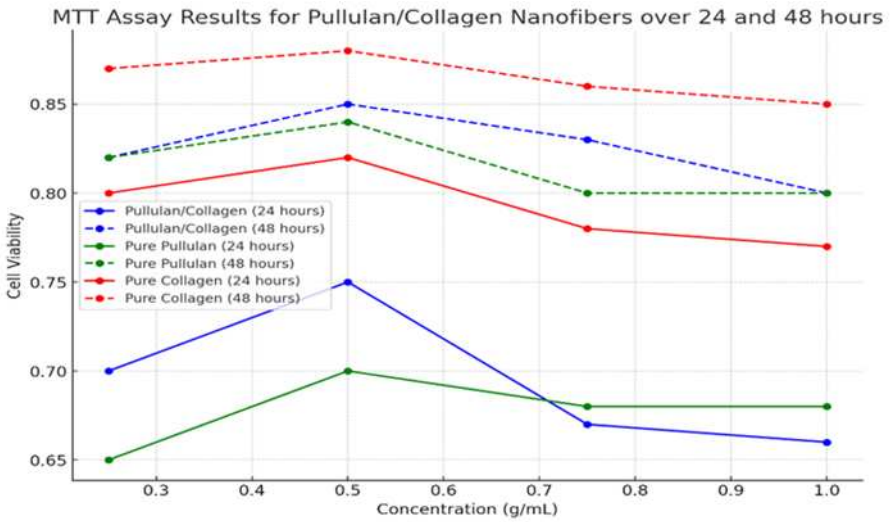

Figure 8. MTT Assay Results for Pullulan/Collagen Nanofibers over 24 and 48 hours.

Preprints (www.preprints.org) | NOT PEER-REVIEWED | Posted: 2 November 2023 doi:10.20944/preprints202311.0115.v1

Table 1. MTT assay was applied to investigate the cell viability at 24 and 48 h.

Concentration (g/mL)	Pullulan/Collagen Cell Viability at 24 hours	Pullulan/Collagen Cell Viability at 48 hours	Pure Pull at 24 hours	Pure Pull at 48 hours	Pure Collagen at 24 hours	Pure Collagen at 48 hours
0.25	0.70	0.82	0.65	0.82	0.80	0.87
0.50	0.75	0.85	0.70	0.84	0.82	0.88
0.75	0.67	0.83	0.68	0.80	0.78	0.86
1.00	0.66	0.80	0.68	0.80	0.77	0.85

Figure 9 plot provides a grouped bar chart for each concentration level (0.25, 0.50, 0.75, 1.00 g/mL). Each group of bars represents the absorbance values at a specific concentration, and each bar within a group corresponds to a different category. This makes it easy to compare the cell viability of the different categories at specific concentrations. The interpretation of the MTT assay results depends on the specific experiment. Typically, higher absorbance values represent higher cell viability, suggesting that the material is less biodegradable. However, it is essential to consider the context of the experiment and other factors that might affect cell viability.

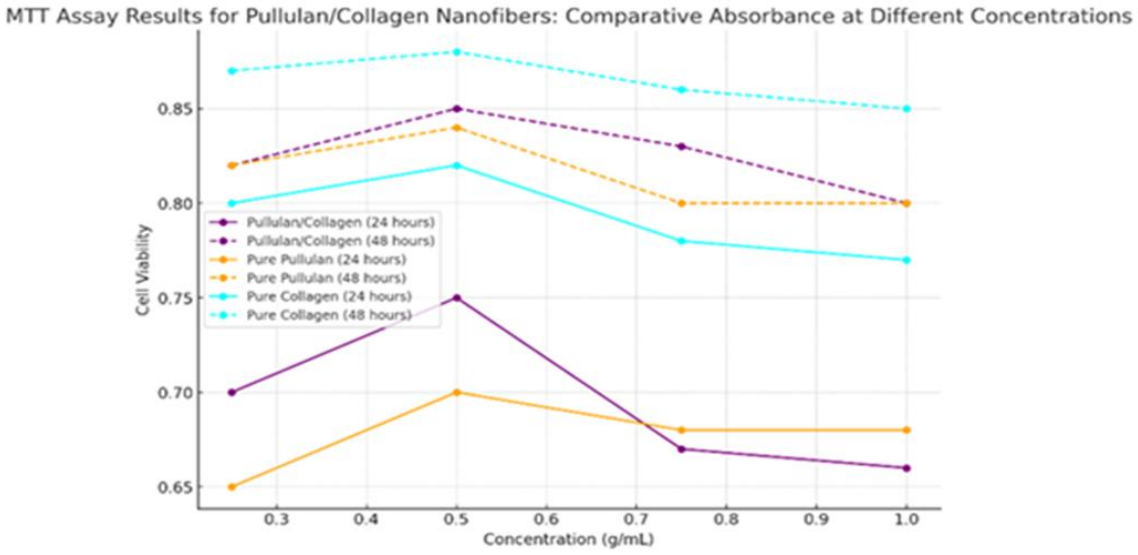

Figure 9. MTT Assay Results for Pullulan/Collagen Nanofibers: Comparative Absorbance at Different Concentrations.

5. Conclusions

The skin plays a vital role as a protective barrier against external factors, emphasizing the need to identify agents that can enhance its function. The prohibition of animal testing for cosmetics has prompted the development of alternative methods to evaluate the safety and effectiveness of

 doi:10.20944/preprints202311.0115.v1

cosmetic ingredients. This study aimed to assess the efficacy of hydroxy acids, including alpha-hydroxy acids (AHA), beta-hydroxy acids (BHA), and polyhydroxy acids (PHA), in acne treatment. Hydroxy acids have demonstrated effectiveness in various skin disorders and have become popular cosmetic ingredients. Glycolic acid, lactic acid, and salicylic acid are commonly used AHAs and BHAs, known for their exfoliating properties and ability to improve skin texture and appearance. The study revealed that high concentrations of hydroxy acids could be toxic, leading to reduced tissue viability. However, lower concentrations of AHAs and PHAs showed positive effects on the organization of the stratum corneum and the expression of skin barrier proteins. PHA exhibited the most significant effects among the hydroxy acids studied due to its hydroxyl groups, chelating properties, moisturizing effect, and antioxidant properties. The objective was to develop a matrix capable of effectively delivering these acids for various skincare applications. The pullulan solution, prepared with a 10% weight percentage in distilled water, was combined with a PVA solution and NaCl to create a stable mixture. The collagen-pullulan solution was prepared by dissolving Collagen and Pullulan in deionized water, mixing, and stirring at 30 °C for 24 hours. Different weight ratios of Collagen to Pullulan, ranging from 25/75 to 50/50, were tested to determine the optimal composition. The encapsulation process involved combining the collagen-pullulan solution with active ingredient solutions containing desired concentrations of AHA and BHA. This mixture was homogenized to ensure a uniform dispersion, and additional processing techniques, such as electrospinning, were utilized to form nanofibers or particles.

The results indicated successful nanofiber preparation, with highly spun, uniform structures observed in several experiments. However, there were instances where the fibres accumulated on the electrode surface, suggesting a need for parameter optimization during spinning. The concentrations of Pullulan at 15% and Collagen at 7.5% also yielded similar results, forming a uniform and porous structure. The characterization of pullulan-collagen-encapsulated AHA-BHA nanofibers was conducted using various analytical techniques. Scanning Electron Microscopy (SEM) images revealed well-formed and continuous nanofibers in acidic solutions, confirming successful electrospinning. However, Pullulan with a neutral to alkaline pH did not exhibit successful electrospinning without a carrier polymer. The nanofibers' average diameter was 33.31643 nm, while the average diameter of the encapsulated particles was 473.6429 nm. Fourier Transform Infrared Spectroscopy (FTIR) analysis provided insights into the chemical bonds and groups present in the nanofiber samples. Absorption peaks at specific wave numbers indicated the presence of ester, carboxylic acid, hydroxyl, and phenolic groups in the nanofibers, depending on the sample composition. Contact angle measurements demonstrated that the pullulan-collagen nanocomposite exhibited hydrophilic properties with a water contact angle 86.90°. The presence of Collagen in the nanocomposite slightly increased its hydrophilicity compared to pure Pullulan, although it remained less hydrophilic than pure Collagen. Biocompatibility assays, specifically the MTT assay, were conducted to evaluate cell viability. The results showed that the pullulan-collagen nanocomposite promoted the highest cell viability for mesenchymal stem cells (MSCs) and human skin fibroblasts (HSFs) at 24 and 48 hours. The appropriate concentration of Pullulan for HSF proliferation was determined to be 0.25 g/mL. Pure collagen fibres at different concentrations also positively affected cell viability, with higher concentrations showing increased viability over time.

These findings highlight the potential of pullulan-collagen-encapsulated AHA-BHA nanofibers for various applications in tissue engineering and regenerative medicine. The successful electrospinning of nanofibers, combined with their chemical composition and hydrophilicity, make them promising candidates for delivering active ingredients in skincare and promoting cell growth and viability.

References

1. Arda O, Göksügür N, Tüzün Y. Basic histological structure and functions of facial skin. Clin Dermatol 2014;32:3–13. https://doi.org/10.1016/j.clindermatol.2013.05.021.
2. Jensen JM, Proksch E. The skin's barrier. G Ital Dermatol Venereol 2009;144:689–700.

3. Kaziga R, Muchunguzi C, Achen D, Kools S. Beauty Is Skin Deep; The Self-Perception of Adolescents and Young Women in Construction of Body Image within the Ankole Society. Int J Environ Res Public Health 2021;18:7840. https://doi.org/10.3390/ijerph18157840.
4. Choi JH, Jin SW, Lee GH, Cho SM, Jeong HG. Orostachys japonicus ethanol extract inhibits 2,4-dinitrochlorobenzene-induced atopic dermatitis-like skin lesions in NC/Nga mice and TNF-α/IFN-γ-induced TARC expression in HaCaT cells. Toxicol Res 2019;36:99–108. https://doi.org/10.1007/s43188-019-00026-0.
5. Reduan FH, Shaari RM, Sayuti NSA, Mustapha NM, Abu Bakar MZ, Sithambaram S, et al. Acute and subacute dermal toxicity of ethanolic extract of Melastoma malabathricum leaves in Sprague-Dawley rats. Toxicol Res 2020;36:203–10. https://doi.org/10.1007/s43188-019-00013-5.
6. Avci P, Sadasivam M, Gupta A, De Melo WC, Huang Y-Y, Yin R, et al. Animal models of skin disease for drug discovery. Expert Opin Drug Discov 2013;8:331–55. https://doi.org/10.1517/17460441.2013.761202.
7. Balls M. Postponement of the EU ban on animal tests for cosmetic ingredients. Altern Lab Anim 1997;25:401–3.
8. Kuehn BM. The EU bans cosmetics testing on animals. J Am Vet Med Assoc 2003;222:559.
9. Dellambra E, Odorisio T, D'Arcangelo D, Failla CM, Facchiano A. Non-animal models in dermatological research. ALTEX 2019;36:177–202. https://doi.org/10.14573/altex.1808022.
10. Agonia AS, Palmeira-de-Oliveira A, Cardoso C, Augusto C, Pellevoisin C, Videau C, et al. Reconstructed Human Epidermis: An Alternative Approach for In Vitro Bioequivalence Testing of Topical Products. Pharmaceutics 2022;14:1554. https://doi.org/10.3390/pharmaceutics14081554.
11. Plaza C, Meyrignac C, Botto J-M, Capallere C. Characterization of a New Full-Thickness In Vitro Skin Model. Tissue Eng Part C Methods 2021;27:411–20. https://doi.org/10.1089/ten.TEC.2021.0035.
12. Zeltinger J, Holbrook KA. A model system for long-term serum-free suspension organ culture of human fetal tissues: experiments on digits and skin from multiple body regions. Cell Tissue Res 1997;290:51–60. https://doi.org/10.1007/s004410050907.
13. Mavon A, Bacqueville D, Wever B. Reconstructed human skin and skin organ culture models used in cosmetic efficacy testing. Handbook of Cosmetic Science and Technology, Third Edition, 2009, p. 345–56.
14. Filaire E, Nachat-Kappes R, Laporte C, Harmand M-F, Simon M, Poinsot C. Alternative in vitro models used in the main safety tests of cosmetic products and new challenges. Int J Cosmet Sci 2022;44:604–13. https://doi.org/10.1111/ics.12803.
15. eBooks.com. Cosmeceuticals and Cosmetic Ingredients. EBooksCom n.d. https://www.ebooks.com/en-cz/book/1189015/cosmeceuticals-and-cosmetic-ingredients/leslie-s-baumann/ (accessed March 2, 2023).
16. Kabene S, Baadel S. Bioethics: a look at animal testing in medicine and cosmetics in the UK. J Med Ethics Hist Med 2019;12:15. https://doi.org/10.18502/jmehm.v12i15.1875.
17. Józsa L, Nemes D, Pető Á, Kósa D, Révész R, Bácskay I, et al. Recent Options and Techniques to Assess Improved Bioavailability: In Vitro and Ex Vivo Methods. Pharmaceutics 2023;15:1146. https://doi.org/10.3390/pharmaceutics15041146.
18. Goddard ED, Gruber JV, editors. Principles of polymer science and technology in cosmetics and personal care. New York: Marcel Dekker; 1999.
19. Baumann L. Cosmetic Dermatology: Principles and Practice, Second Edition. Mcgraw-hill; 2009.
20. Debeer S, Le Luduec J-B, Kaiserlian D, Laurent P, Nicolas J-F, Dubois B, et al. Comparative histology and immunohistochemistry of porcine versus human skin. Eur J Dermatol 2013;23:456–66. https://doi.org/10.1684/ejd.2013.2060.
21. Ba G, Rj Y, Ej VS. Clinical and cosmeceutical uses of hydroxyacids. Clinics in Dermatology 2009;27. https://doi.org/10.1016/j.clindermatol.2009.06.023.
22. Yu RJ, Van Scott EJ. Hydroxycarboxylic acids, N-acetylamino sugars, and N-acetylamino acids. Skinmed 2002;1:117–22; quiz 125–6. https://doi.org/10.1111/j.1540-9740.2002.01646a.x.
23. Kornhauser A, Coelho SG, Hearing VJ. Effects of Cosmetic Formulations Containing Hydroxyacids on Sun-Exposed Skin: Current Applications and Future Developments. Dermatol Res Pract 2012;2012:710893. https://doi.org/10.1155/2012/710893.
24. Rostkowska E, Poleszak E, Wojciechowska K, Dos Santos Szewczyk K. Dermatological Management of Aged Skin. Cosmetics 2023;10:55. https://doi.org/10.3390/cosmetics10020055.
25. Mawazi SM, Ann J, Othman N, Khan J, Alolayan SO, Al thagfan SS, et al. A Review of Moisturizers; History, Preparation, Characterization and Applications. Cosmetics 2022;9:61. https://doi.org/10.3390/cosmetics9030061.
26. Milosheska D, Roškar R. Use of Retinoids in Topical Antiaging Treatments: A Focused Review of Clinical Evidence for Conventional and Nanoformulations. Adv Ther 2022;39:5351–75. https://doi.org/10.1007/s12325-022-02319-7.
27. Zhou H, Luo D, Chen D, Tan X, Bai X, Liu Z, et al. Current Advances of Nanocarrier Technology-Based Active Cosmetic Ingredients for Beauty Applications. Clin Cosmet Investig Dermatol 2021;14:867–87. https://doi.org/10.2147/CCID.S313429.

28. Alpha Hydroxy Acid (AHA) / Beta Hydroxy Acid (BHA), 2010.
29. Tran D, Townley JP, Barnes TM, Greive KA. An antiaging skin care system containing alpha hydroxy acids and vitamins improves the biomechanical parameters of facial skin. Clin Cosmet Investig Dermatol 2014;8:9–17. https://doi.org/10.2147/CCID.S75439.
30. Dayal S, Kaur R, Sahu P. Efficacy of Microneedling With 35% Glycolic Acid Peels Versus Microneedling With 15% Trichloroacetic Acid Peels in Treatment of Atrophic Acne Scars: A Randomized Controlled Trial. Dermatol Surg 2022;48:1203–9. https://doi.org/10.1097/DSS.0000000000003556.
31. Thawabteh AM, Jibreen A, Karaman D, Thawabteh A, Karaman R. Skin Pigmentation Types, Causes and Treatment—A Review. Molecules 2023;28:4839. https://doi.org/10.3390/molecules28124839.
32. Lee H-S, Kim I-H. Salicylic acid peels for the treatment of acne vulgaris in Asian patients. Dermatol Surg 2003;29:1196–9; discussion 1199. https://doi.org/10.1111/j.1524-4725.2003.29384.x.
33. Endly DC, Miller RA. Oily Skin: A review of Treatment Options. J Clin Aesthet Dermatol 2017;10:49–55.
34. Makrantonaki E, Ganceviciene R, Zouboulis C. An update on the role of the sebaceous gland in the pathogenesis of acne. Dermatoendocrinol 2011;3:41–9. https://doi.org/10.4161/derm.3.1.13900.
35. Zheng Y, Liang H, Zhou M, Song L, He C. Skin bacterial structure of young females in China: The relationship between skin bacterial structure and facial skin types. Exp Dermatol 2021;30:1366–74. https://doi.org/10.1111/exd.14105.
36. Goodman G. Cleansing and moisturizing in acne patients. Am J Clin Dermatol 2009;10 Suppl 1:1–6. https://doi.org/10.2165/0128071-200910001-00001.
37. Tang S-C, Yang J-H. Dual Effects of Alpha-Hydroxy Acids on the Skin. Molecules 2018;23:863. https://doi.org/10.3390/molecules23040863.
38. Oge' LK, Broussard A, Marshall MD. Acne Vulgaris: Diagnosis and Treatment. Am Fam Physician 2019;100:475–84.
39. Hwang J, Jeong H, Lee N, Hur S, Lee N, Han JJ, et al. Ex Vivo Live Full-Thickness Porcine Skin Model as a Versatile In Vitro Testing Method for Skin Barrier Research. International Journal of Molecular Sciences 2021;22:657. https://doi.org/10.3390/ijms22020657.
40. Sabzevari N, Qiblawi S, Norton S, Fivenson D. Sunscreens: UV filters to protect us: Part 1: Changing regulations and choices for optimal sun protection. International Journal of Women's Dermatology 2021;7:28–44. https://doi.org/10.1016/j.ijwd.2020.05.017.
41. Tahir R, Albargi HB, Ahmad A, Qadir MB, Khaliq Z, Nazir A, et al. Development of Sustainable Hydrophilic Azadirachta indica Loaded PVA Nanomembranes for Cosmetic Facemask Applications. Membranes (Basel) 2023;13:156. https://doi.org/10.3390/membranes13020156.
42. Dayan N. 4 - Delivery System Design in Topically Applied Formulations: An Overview. In: Rosen MR, editor. Delivery System Handbook for Personal Care and Cosmetic Products, Norwich, NY: William Andrew Publishing; 2005, p. 101–18. https://doi.org/10.1016/B978-081551504-3.50009-2.
43. Cimini A, Imperi E, Picano A, Rossi M. Electrospun nanofibers for medical face mask with protection capabilities against viruses: State of the art and perspective for industrial scale-up. Appl Mater Today 2023;32:101833. https://doi.org/10.1016/j.apmt.2023.101833.
44. Aguilar-Toalá JE, Quintanar-Guerrero D, Liceaga AM, Zambrano-Zaragoza ML. Encapsulation of bioactive peptides: a strategy to improve the stability, protect the nutraceutical bioactivity and support their food applications. RSC Adv n.d.;12:6449–58. https://doi.org/10.1039/d1ra08590e.
45. Pacheco G, Mello C, Chiari-Andréo B, Isaac V, Ribeiro S, Pecoraro E, et al. Bacterial cellulose skin masks—Properties and sensory tests. Journal of Cosmetic Dermatology 2017;17. https://doi.org/10.1111/jocd.12441.
46. Quattrone A, Czajka A, Sibilla S. Thermosensitive Hydrogel Mask Significantly Improves Skin Moisture and Skin Tone; Bilateral Clinical Trial. Cosmetics 2017;4:17. https://doi.org/10.3390/cosmetics4020017.
47. Huang C, Xu X, Fu J, Yu D-G, Liu Y. Recent Progress in Electrospun Polyacrylonitrile Nanofiber-Based Wound Dressing. Polymers (Basel) 2022;14:3266. https://doi.org/10.3390/polym14163266.
48. Shen R, Guo Y, Wang S, Tuerxun A, He J, Bian Y. Biodegradable Electrospun Nanofiber Membranes as Promising Candidates for the Development of Face Masks. International Journal of Environmental Research and Public Health 2023;20:1306. https://doi.org/10.3390/ijerph20021306.
49. Rahman MZ, Hoque ME, Alam MR, Rouf MA, Khan SI, Xu H, et al. Face Masks to Combat Coronavirus (COVID-19)—Processing, Roles, Requirements, Efficacy, Risk and Sustainability. Polymers (Basel) 2022;14:1296. https://doi.org/10.3390/polym14071296.
50. Essa WK, Yasin SA, Saeed IA, Ali GAM. Nanofiber-Based Face Masks and Respirators as COVID-19 Protection: A Review. Membranes 2021;11. https://doi.org/10.3390/membranes11040250.
51. Zare M, Dziemidowicz K, Williams GR, Ramakrishna S. Encapsulation of Pharmaceutical and Nutraceutical Active Ingredients Using Electrospinning Processes. Nanomaterials (Basel) 2021;11:1968. https://doi.org/10.3390/nano11081968.
52. Naragund VS, Panda PK. Electrospun nanofiber-based respiratory face masks—a review. Emergent Mater 2022;5:261–78. https://doi.org/10.1007/s42247-022-00350-6.

53. Rodan K, Fields K, Majewski G, Falla T. Skincare Bootcamp: The Evolving Role of Skincare. Plast Reconstr Surg Glob Open 2016;4:e1152. https://doi.org/10.1097/GOX.0000000000001152.
54. Wang X. A theory for the mechanism of action of the alpha-hydroxy acids applied to the skin. Med Hypotheses 1999;53:380–2. https://doi.org/10.1054/mehy.1998.0788.
55. Wang X. A theory for the mechanism of homocysteine-induced vascular pathogenesis. Medical Hypotheses 1999;53:386–94. https://doi.org/10.1054/mehy.1998.0787.
56. Okano Y, Abe Y, Masaki H, Santhanam U, Ichihashi M, Funasaka Y. Biological effects of glycolic acid on dermal matrix metabolism mediated by dermal fibroblasts and epidermal keratinocytes. Exp Dermatol 2003;12 Suppl 2:57–63. https://doi.org/10.1034/j.1600-0625.12.s2.9.x.
57. Bernstein EF, Lee J, Brown DB, Yu R, Van Scott E. Glycolic acid treatment increases type I collagen mRNA and hyaluronic acid content of human skin. Dermatol Surg 2001;27:429–33. https://doi.org/10.1046/j.1524-4725.2001.00234.x.
58. Rendl M, Mayer C, Weninger W, Tschachler E. Topically applied lactic acid increases spontaneous secretion of vascular endothelial growth factor by human reconstructed epidermis. Br J Dermatol 2001;145:3–9. https://doi.org/10.1046/j.1365-2133.2001.04274.x.